Hadron production and spectroscopy at ATLAS

Konstantin Toms
on behalf of the ATLAS Collaboration

University of New Mexico

Outline

- ATLAS has a rich program for studies of hadron production and spectroscopy.
- Selected results covered in this talk:
  - $B_c(2S)$ observation
  - Study of the $B_c^+ \to J/\psi D_s^+$ and $B_c^+ \to J/\psi D_s^{*+}$ decays
  - Search for the X_b and other hidden-beauty states
  - Measurement of the branching ratio $\Gamma(\Lambda_b^0 \to \psi(2S)\Lambda^0)/\Gamma(\Lambda_b^0 \to J/\psi\Lambda^0)$
  - Production measurements of $\psi(2S)$ and $X(3872)$
- https://twiki.cern.ch/twiki/bin/view/AtlasPublic/BPhysPublicResults
- Much more to come soon!

$B_c(2S)$ observation

- Phys. Rev. Lett. **113**, 212004 (2014)

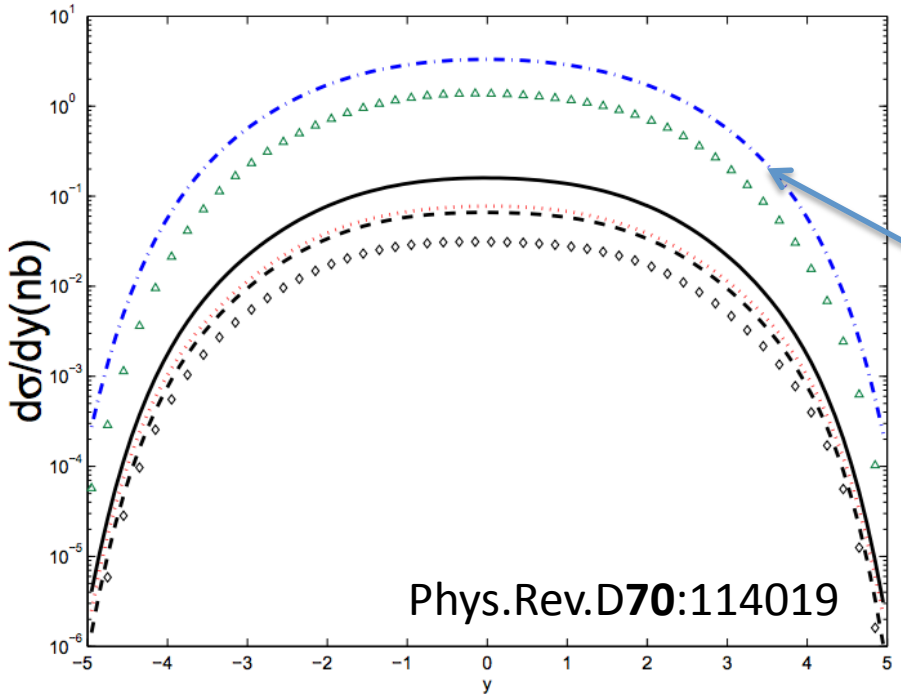

Ground state: $B^{\pm}_c \rightarrow J/\Psi(\mu^+\mu^-)\,\pi^{\pm}$

Peak is observed in the mass difference distribution $m(B^{\pm}_c(2S)) - m(B^{\pm}_c) - 2m(\pi^{\pm})$

- B_c is a unique system: two distinct heavy quarks.
- "Intermediate" between the $b\bar{b}$ and $c\bar{c}$.
- Many theoretical predictions for the bc-family spectroscopy and production properties.
- Production is predicted to be suppressed in the forward-backward regions (various excited states).

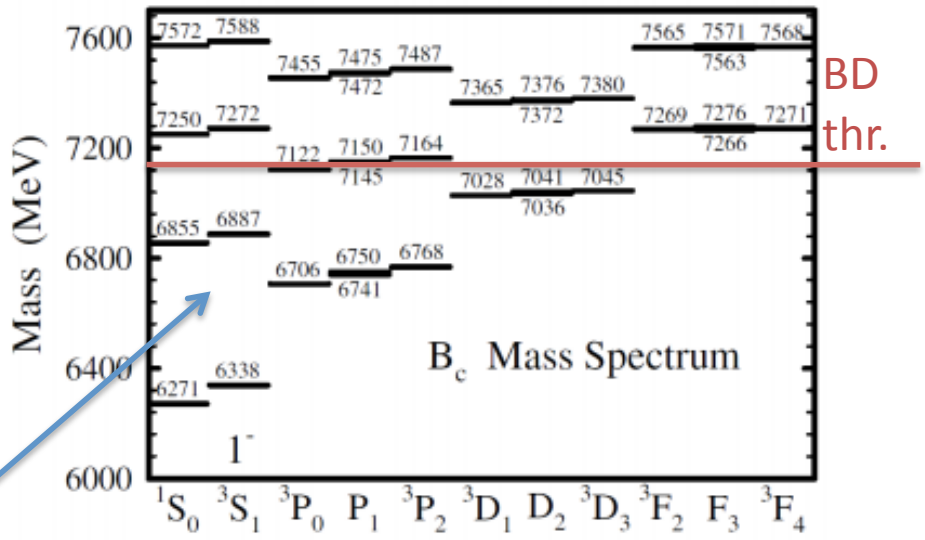

S. Godfrey, PRD 70, 054017(2004)

$B_c(2S)$, cont.

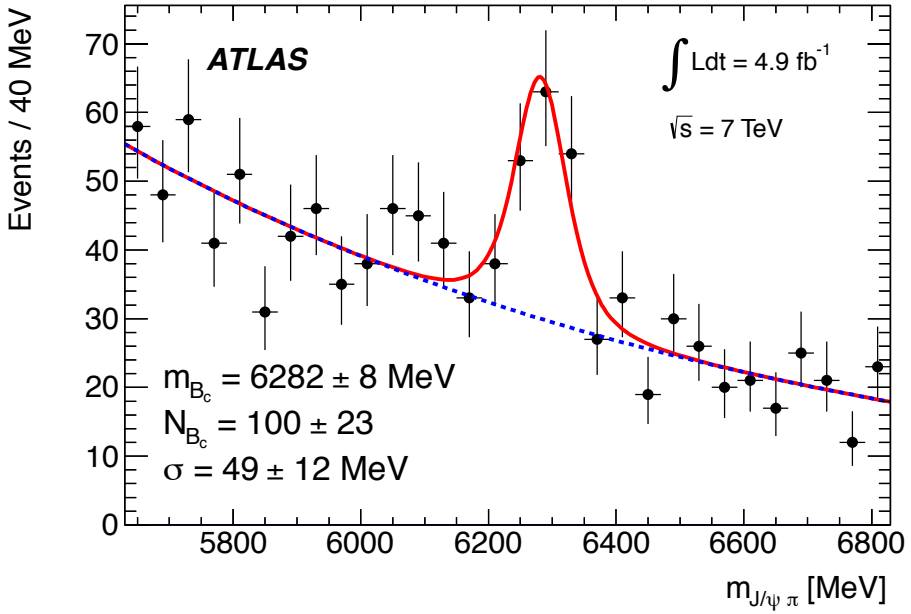

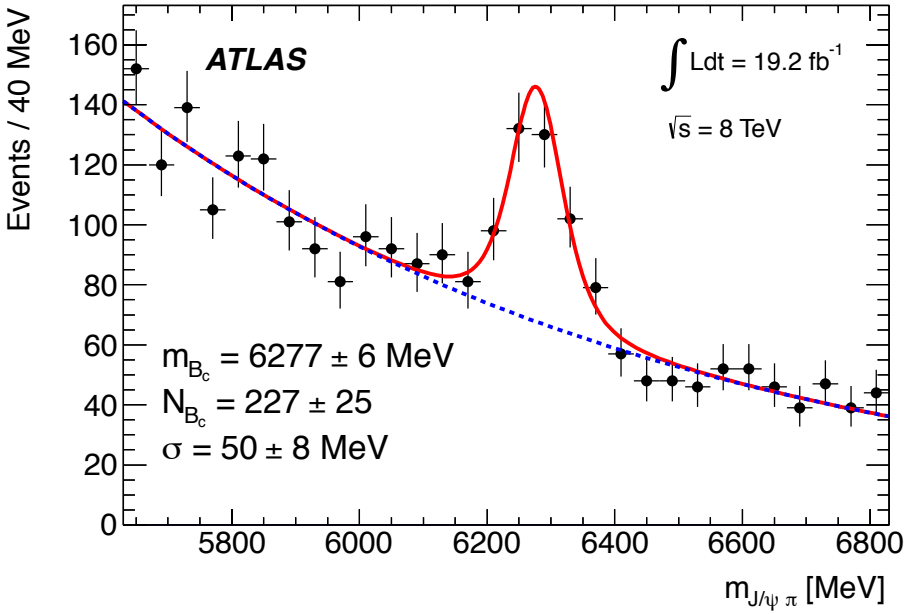

- Ground state: $B^{\pm}_c \rightarrow J/\Psi(\mu^+\mu^-)\,\pi^{\pm}$

$B_c(2S)$, cont.

- First observation of the excited B_c state, the $B_c(2S)$.
- Mass of the peak m[$B_c(2S)$]= $6842 \pm 4_{stat} \pm 5_{syst}$ MeV is consistent with the theory [6835-6917], as well as the decay mode.
- The observed yield is within the theoretical expectations.
- 5.2 sigma observation for the combination of 7 and 8 TeV datasets (LEE included, local is 5.4).
- Further studies possible with new data.

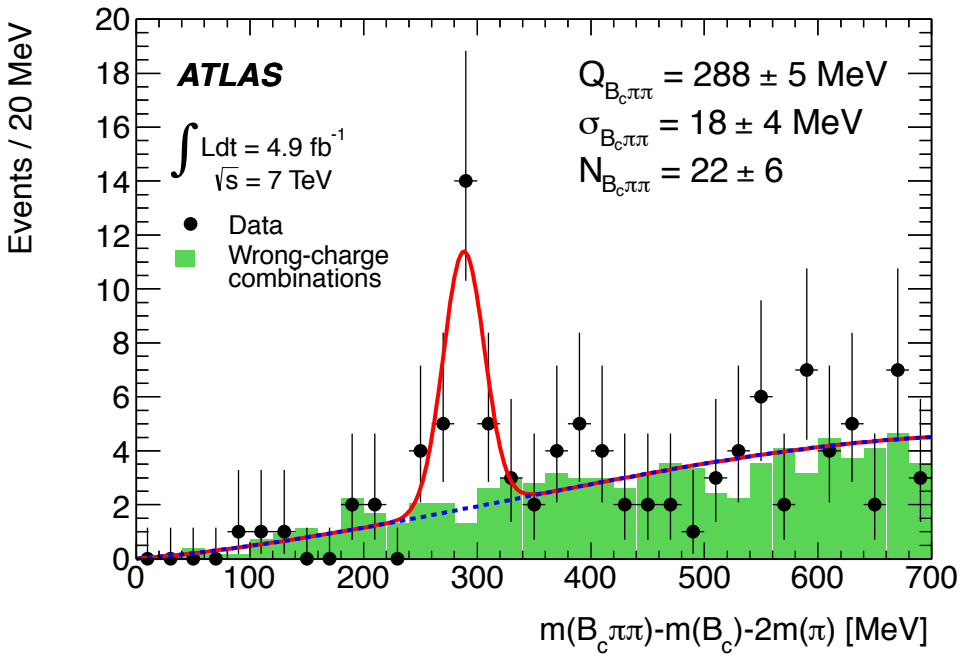

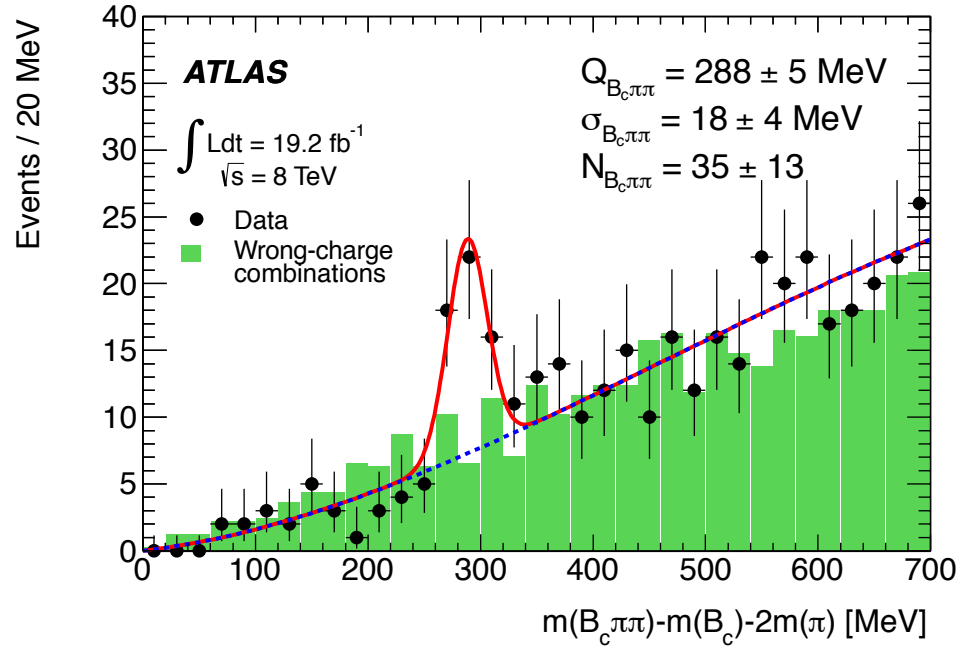

Study of the $B_c^+ \to J/\psi D_s^+$ and $B_c^+ \to J/\psi D_s^{*+}$ decays

- Eur. Phys. J. C, 76(1), 1 (2016).
- $\bar{b}c \to c\bar{c}c\bar{s}$ transition:

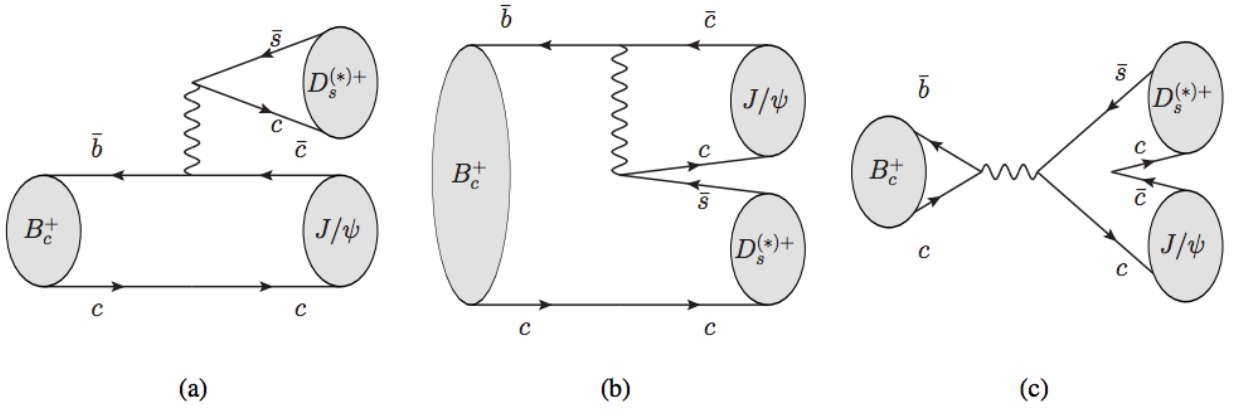

Figure 1: Feynman diagrams for $B_c^+ \to J/\psi D_s^{(*)+}$ decays: (a) colour-favoured spectator, (b) colour-suppressed spectator, and (c) annihilation topology.

- Measurement of the relative branching fractions of $B_c^+ \to J/\psi D_s^+$ and $B_c^+ \to J/\psi D_s^{*+}$ and of the branching fractions relative to $B_c^+ \to J/\psi \pi^+$ decay.
- $D_s^{*+} \to D_s^+ [\pi^0/\gamma]_{soft}$, $D_s^+ \to \varphi(K^+K^-)\pi^+$.
- The decay $B_c^+ \to J/\psi D_s^{*+}$ is a transition of a pseudoscalar meson into a pair of vector states and is thus described by the three helicity amplitudes, A_{++}, A_{--}, and A_{00}.
- The contribution of the A_{++} and A_{--} amplitudes, referred to as the $A_{\pm\pm}$ component, corresponds to the J/ψ and D_s^{*+} transverse polarisation.
- Measurement of the fraction of transverse polarisation, $\Gamma_{\pm\pm}/\Gamma = \Gamma_{\pm\pm}(B_c^+ \to J/\psi D_s^{*+})/\Gamma(B_c^+ \to J/\psi D_s^{*+})$. From the naïve spin model should be 2/3.

Study of the $B_c^+ \to J/\psi D_s^+$ and $B_c^+ \to J/\psi D_s^{*+}$ decays, results (1)

- 2D unbinned maximum likelihood fit of B_c^+ invariant mass and helicity angle $\theta'(\mu^+)$.

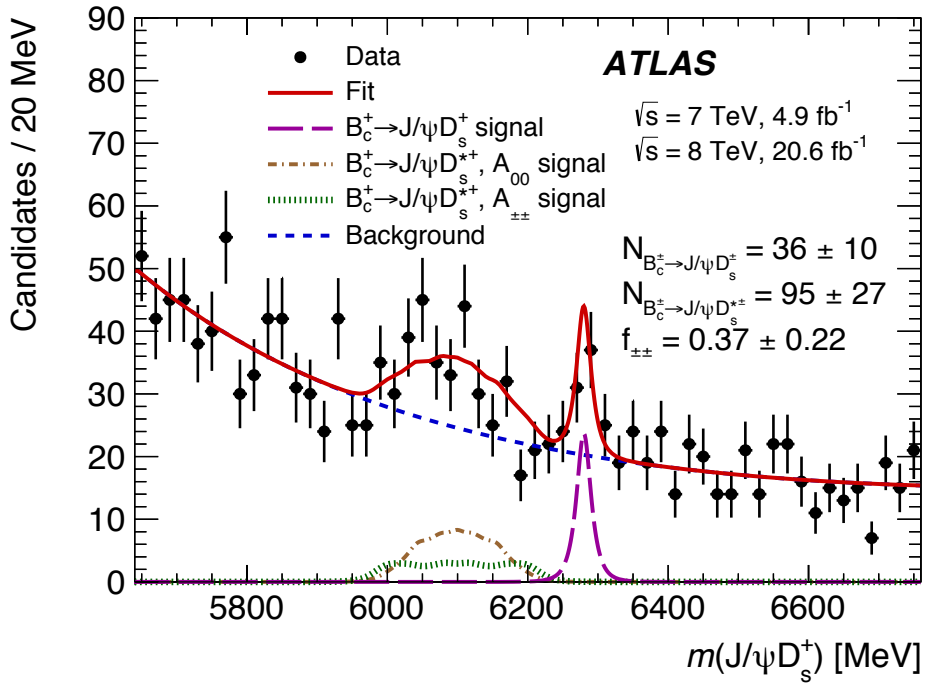

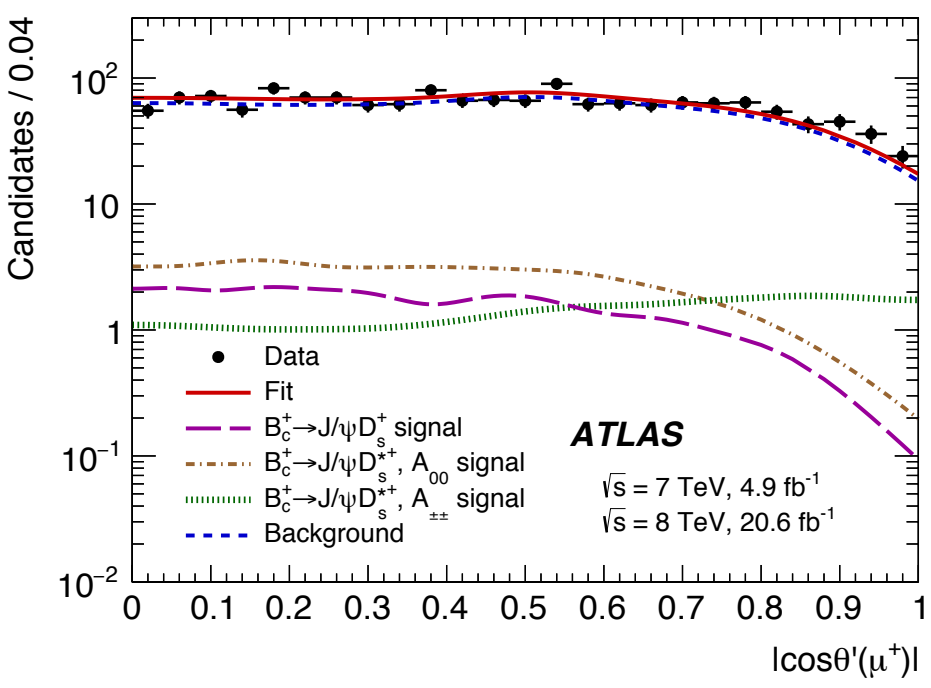

- Measured transverse polarisation fraction $\Gamma_{\pm\pm}/\Gamma = \Gamma_{\pm\pm}(B_c^+ \to J/\psi D_s^{*+})/\Gamma(B_c^+ \to J/\psi D_s^{*+})$

$$\Gamma_{\pm\pm}/\Gamma = 0.38 \pm 0.23\ (\text{stat.}) \pm 0.07\ (\text{syst.})$$

Study of the $B_c^+ \to J/\psi D_s^+$ and $B_c^+ \to J/\psi D_s^{*+}$ decays, results (2)

- Ratios of the branching fractions:

$$\mathcal{R}_{D_s^+/\pi^+} = \frac{\mathcal{B}_{B_c^+ \to J/\psi D_s^+}}{\mathcal{B}_{B_c^+ \to J/\psi \pi^+}} = 3.8 \pm 1.1\ (\text{stat.}) \pm 0.4\ (\text{syst.}) \pm 0.2\ (\text{BF}),$$

$$\mathcal{R}_{D_s^{*+}/\pi^+} = \frac{\mathcal{B}_{B_c^+ \to J/\psi D_s^{*+}}}{\mathcal{B}_{B_c^+ \to J/\psi \pi^+}} = 10.4 \pm 3.1\ (\text{stat.}) \pm 1.5\ (\text{syst.}) \pm 0.6\ (\text{BF}),$$

$$\mathcal{R}_{D_s^{*+}/D_s^+} = \frac{\mathcal{B}_{B_c^+ \to J/\psi D_s^{*+}}}{\mathcal{B}_{B_c^+ \to J/\psi D_s^+}} = 2.8^{+1.2}_{-0.8}\ (\text{stat.}) \pm 0.3\ (\text{syst.})$$

- (BF) corresponds to $Br(D_s^+ \to \phi(K^+K^-)\pi^+)$
- Comparison with theory:

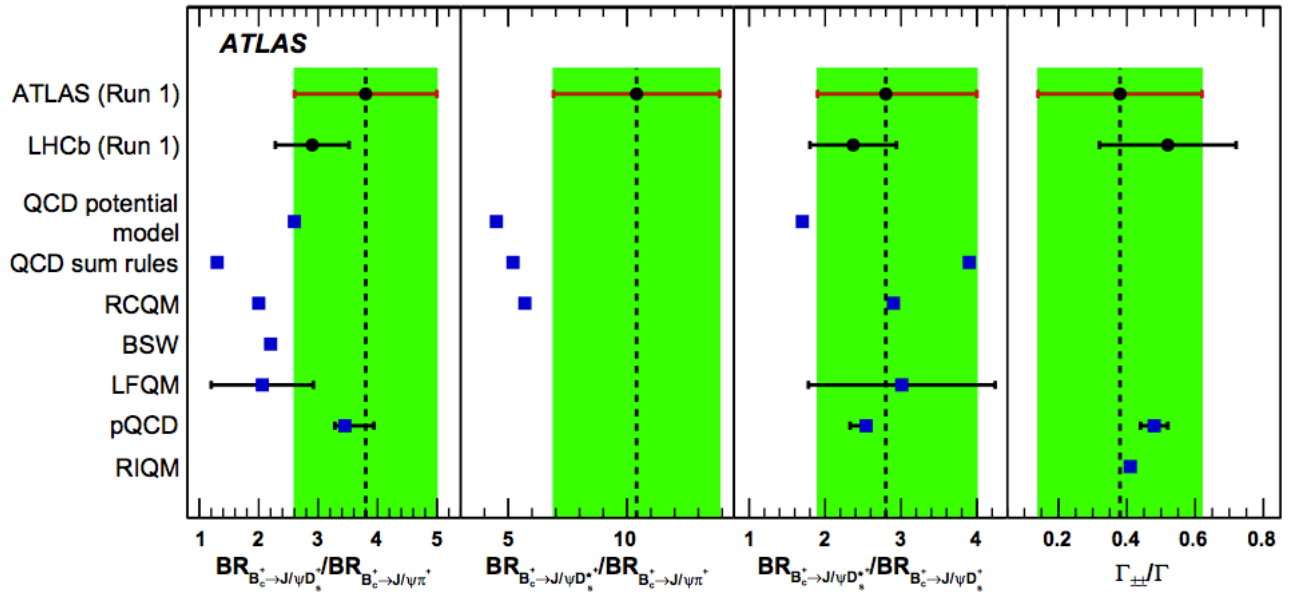

Search for the X_b and other hidden-beauty states at ATLAS (1)

- **Physics Letters B 740 (2015), pp. 199–217**
- 16.2 fb^{-1} of 8 TeV ATLAS data.
- Search in the decay channel $X_b \rightarrow \pi^+ \pi^- \Upsilon(1S)(\rightarrow \mu^+ \mu^-)$.
- Analysis is performed in eight bins of rapidity, transverse momentum, and the angle (in the rest frame of the parent state) between the dipion system and the laboratory-frame momentum of the parent.

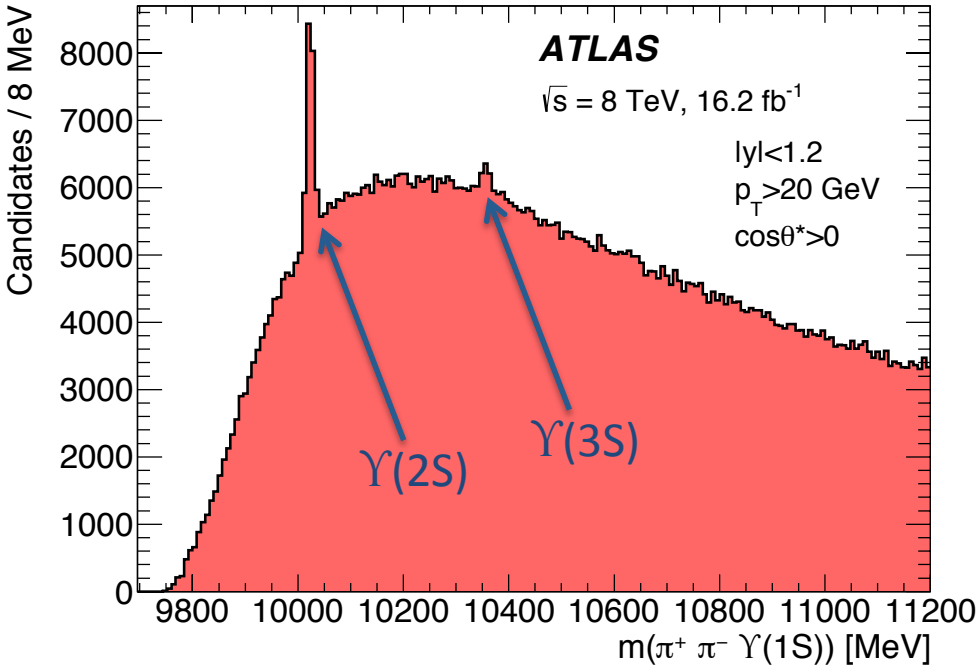

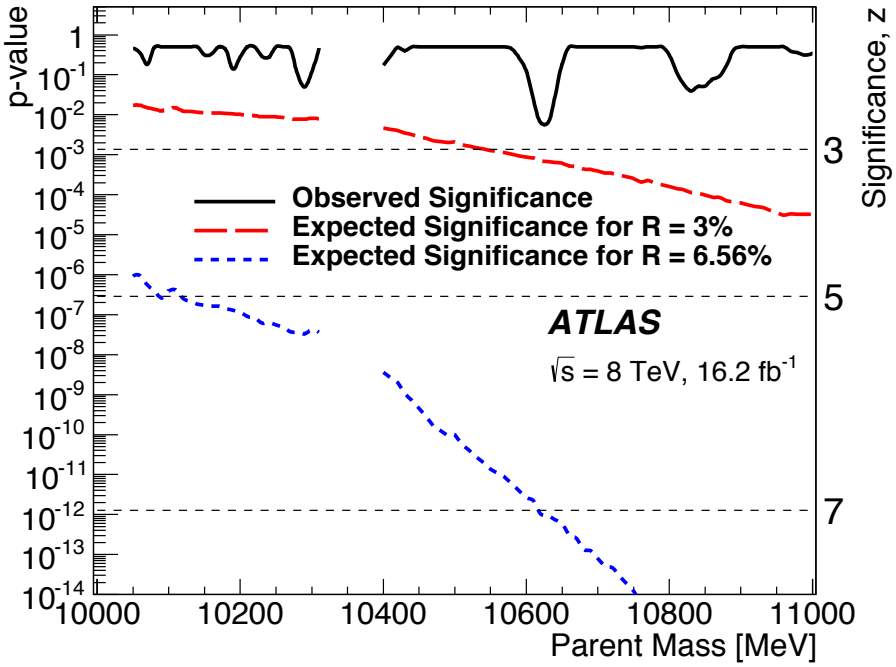

Search for the X_b and other hidden-beauty states at ATLAS (2)

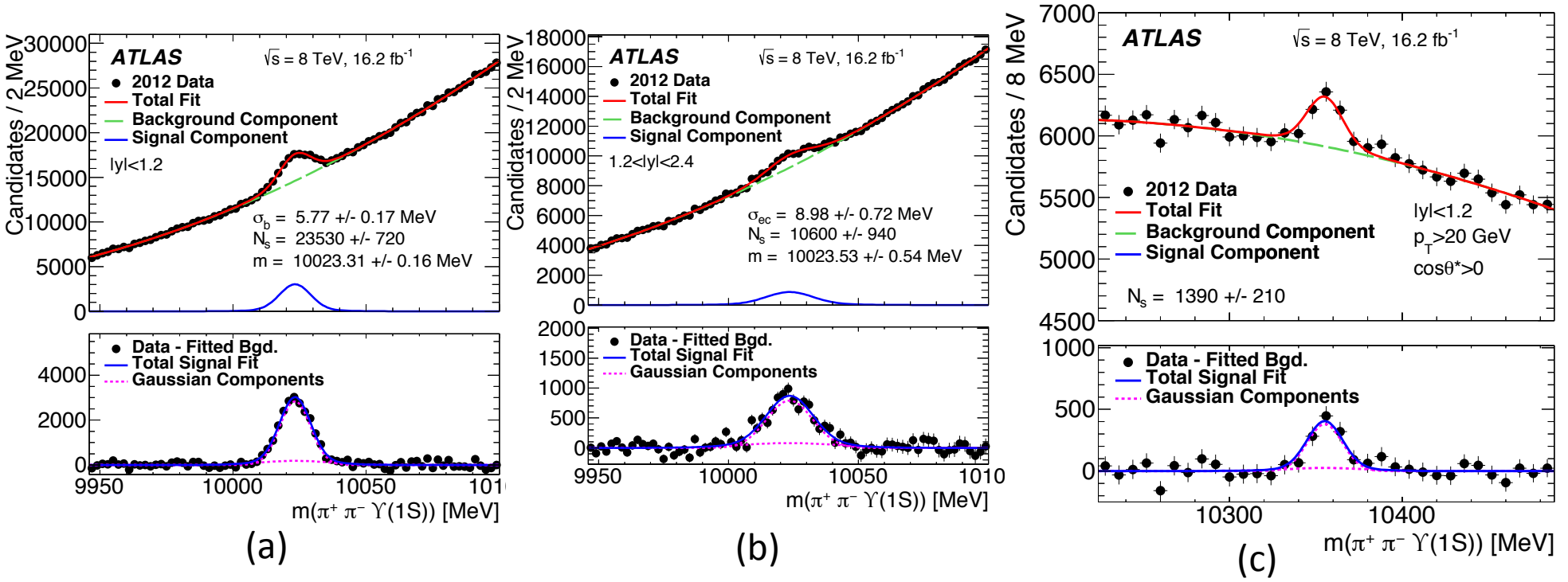

- The signal shape, distribution of signal among analysis bins, and efficiency, are first calibrated on the $\Upsilon(2S)$ peak in data → that it turns out only one parameter: the division of signal between barrel and endcap that needs to be adjusted.
- After this, the simultaneous fit to the 8 bins is validated on the $\Upsilon(3S)$.
- Both the expected overall yield and the division among bins are reproduced well.

Search for the X_b and other hidden-beauty states at ATLAS (3)

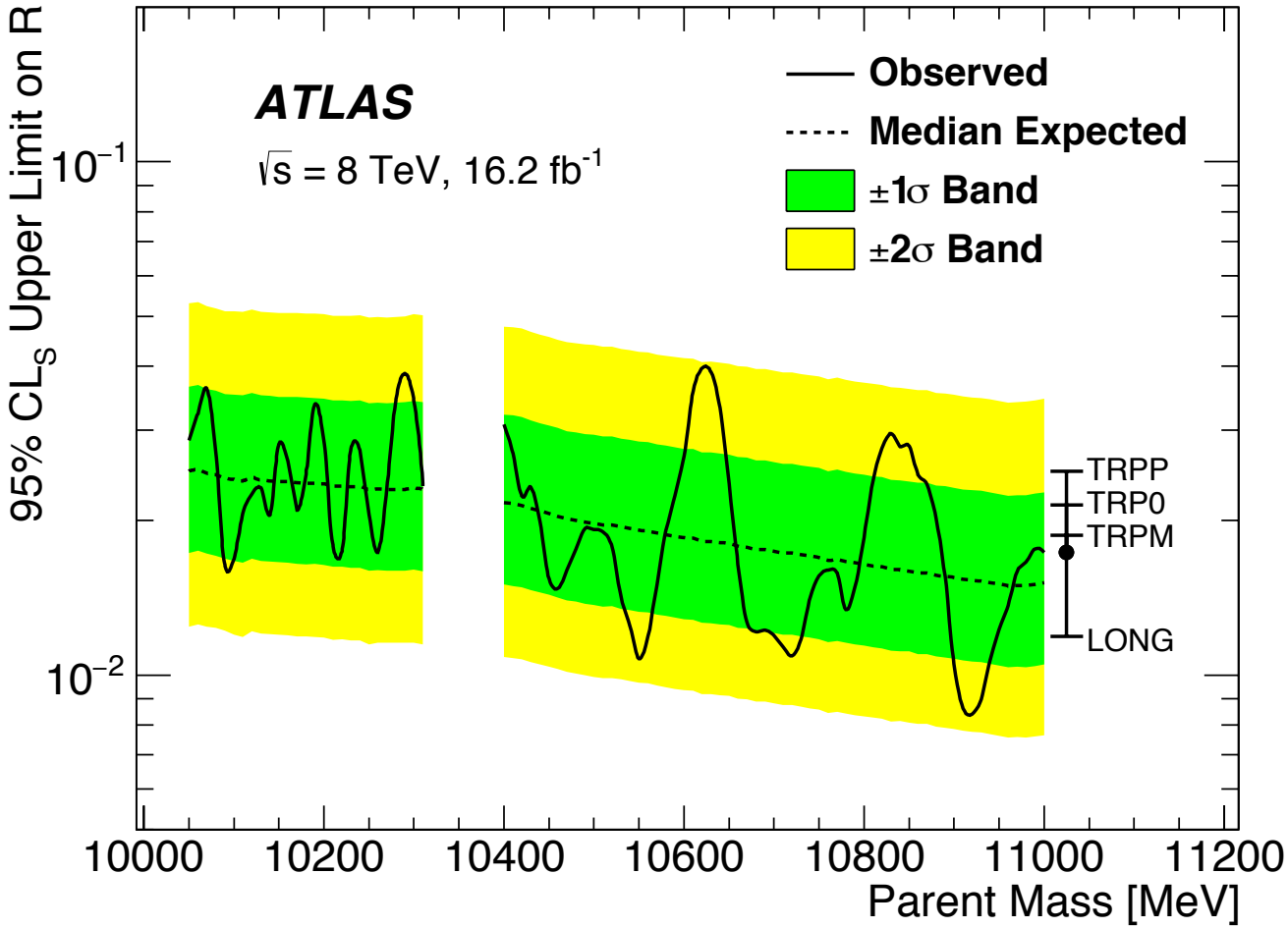

- The bar on the right shows typical shifts under alternative X_b spin-alignment scenarios.
- Upper limits are recalculated under longitudinal ('LONG') and three transverse ('TRPP', 'TRP0', 'TRPM') spin-alignment scenarios.

- No evidence for new narrow states is found for masses 10.05–10.31 GeV and 10.40–11.00 GeV.
- Upper limits are also set on the ratio
  $R = [\sigma(pp \to X_b)\, B(X_b \to \pi^+\pi^-\Upsilon(1S))] \,/\, [\sigma(pp \to \Upsilon(2S))\, B(\Upsilon(2S) \to \pi^+\pi^-\Upsilon(1S))]$,
  with results ranging from 0.8% to 4.0% depending on the X_b mass.

Measurement of the branching ratio $\Gamma(\Lambda_b^0 \to \psi(2S)\Lambda^0)/\Gamma(\Lambda_b^0 \to J/\psi\Lambda^0)$

- Physics Letters B 751 (2015) pp. 63-80.
- 20.6 fb^{-1} of 8 TeV data.
- First observation of $\Lambda_b^0 \to \psi(2S)\Lambda^0$ decay.

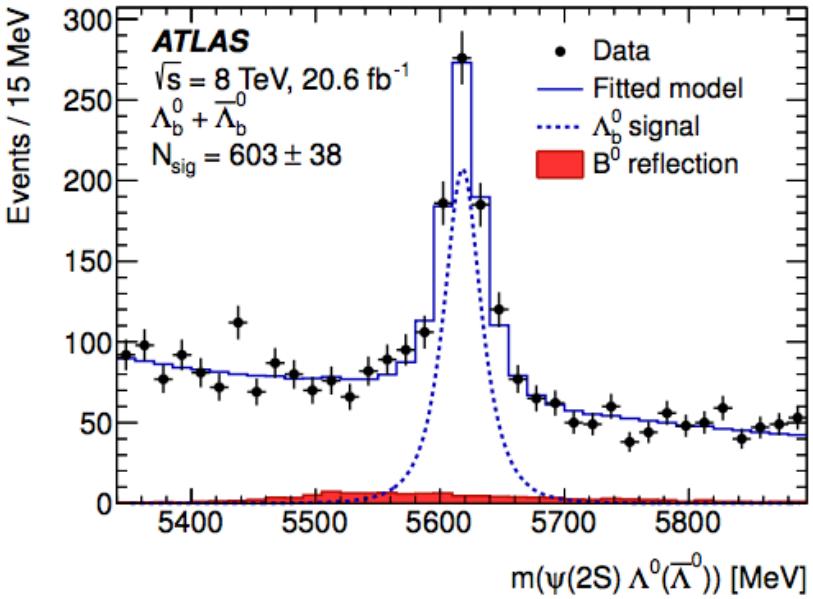

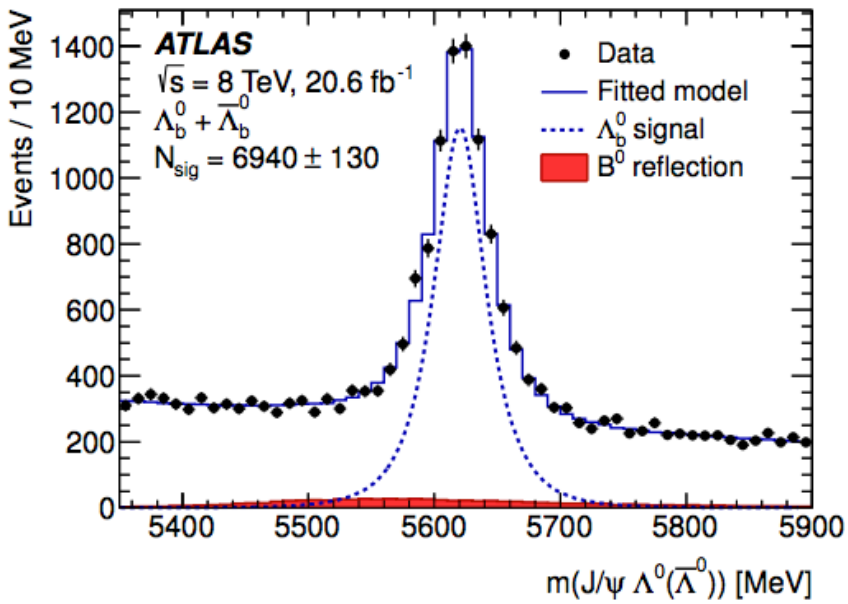

Measurement of the branching ratio $\Gamma(\Lambda_b^0 \to \psi(2S)\Lambda^0)/\Gamma(\Lambda_b^0 \to J/\psi\Lambda^0)$

- Fiducial range: $p_T(\Lambda_b^0) > 10\,\text{GeV},\ |\eta(\Lambda_b^0)| < 2.1$
- The relative branching ratio is calculated as

$$\frac{\Gamma(\Lambda_b^0 \to \psi(2S)\Lambda^0)}{\Gamma(\Lambda_b^0 \to J/\psi\Lambda^0)} = \frac{N_{\text{cor}}(\Lambda_b^0 \to \psi(\mu^+\mu^-)\Lambda^0)}{N_{\text{cor}}(\Lambda_b^0 \to J/\psi(\mu^+\mu^-)\Lambda^0)} \cdot \frac{\mathcal{B}(J/\psi \to \ell^+\ell^-)}{\mathcal{B}(\psi(2S) \to \ell^+\ell^-)}$$

- Where the N_{cor} is the MC-corrected yield.
- Results in:

$$\frac{\Gamma(\Lambda_b^0 \to \psi(2S)\Lambda^0)}{\Gamma(\Lambda_b^0 \to J/\psi\,\Lambda^0)} = 0.501 \pm 0.033(\text{stat}) \pm 0.016(\text{syst}) \pm 0.011(\mathcal{B})$$

- Which is lower than the theoretical prediction of 0.8±0.1 from PRD **88** (2013) 114018 and PRD **92** (2015) 114008.

Production measurements of ψ(2S) and X(3872) at ATLAS (1)

- **JHEP01 (2017) 117**
- Decay mode: $J/\psi\,\pi^+\pi^-$, 11.4 fb^{-1} of 8 TeV ATLAS data.
- Rapidity range $|y|<0.75$, p_T range of $J/\psi\,\pi^+\pi^-$ = (10 – 70) GeV.
- MC simulation is used for studies of selection and reconstruction efficiencies.

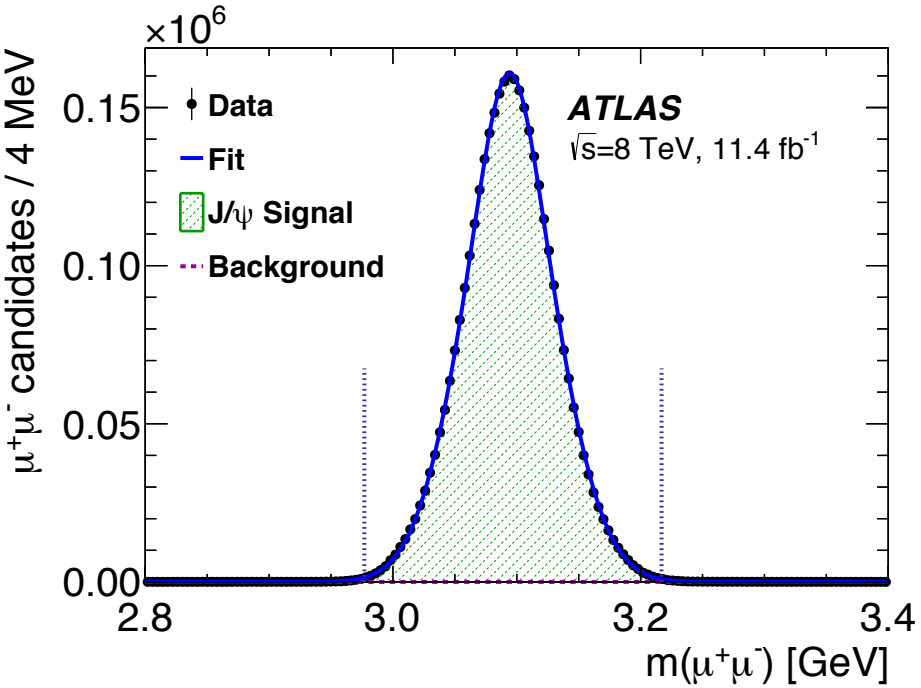

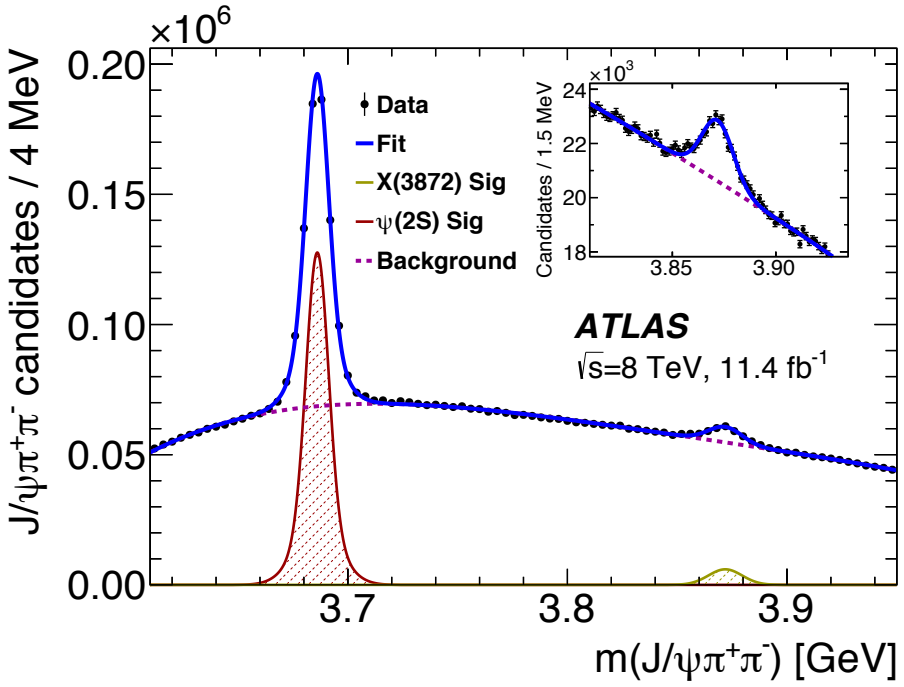

Production measurements of ψ(2S) and X(3872) at ATLAS (2)

- The production cross sections of the ψ(2S) and X(3872) states are measured in five bins of $J/\psi\pi^+\pi^-$ p_T, with bin boundaries
  - (10, 12, 16, 22, 40, 70) GeV.
- The cross sections measured are obtained under the assumption of
  - no spin alignment, but
  - appropriate sets of correction factors for a number of extreme spin alignment scenarios are calculated and presented in the Appendix of the corresponding Conference Note.
- In order to separate prompt production of the ψ(2S) and X(3872) states and the non-prompt production from the decays of long-lived particles such as b-hadrons, the data sample in each p_T bin was divided into intervals of pseudo-proper lifetime $\tau=L_{xy}m/p_T$.
- Four intervals of $\tau(J/\psi\pi^+\pi^-)$ were defined:
  - -0.3 ps $< \tau <$ 0.025 ps
  - 0.025 ps $< \tau <$ 0.3 ps
  - 0.3 ps $< \tau <$ 1.5 ps
  - 1.5 ps $< \tau <$ 15.0 ps

Production measurements of ψ(2S) and X(3872) at ATLAS (3)

- Measured effective pseudo-proper lifetimes for non-prompt X(3872) and ψ(2S), and the ratio of non-prompt X(3872) and ψ(2S) production.

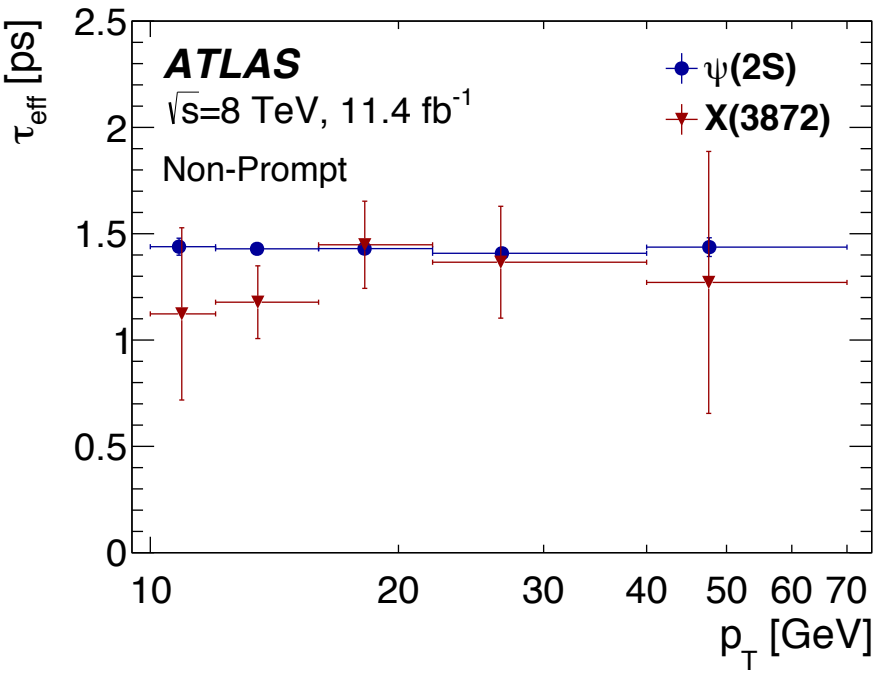

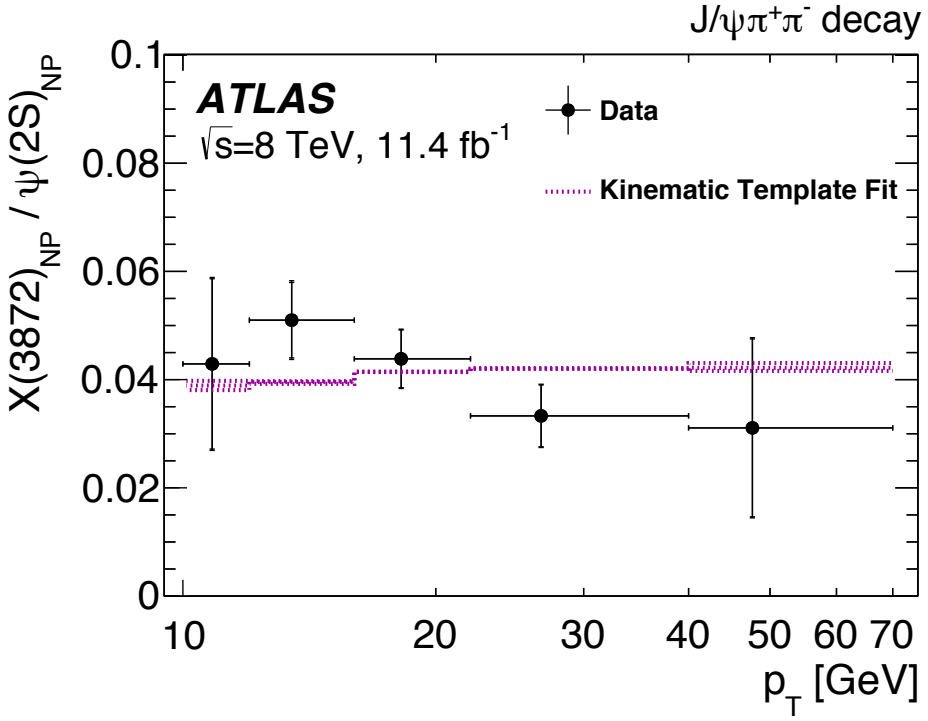

- Kinematic template fit was calculated as a ratio of the simulated p_T distributions of non-prompt X(3872) and non-prompt ψ(2S), assuming that the same mix of the parent b-hadrons contributes for both signals.
- The shape of the template reflects the kinematics of the decay of a b-hadron into ψ(2S) or X(3872), with the width of the band showing the range of variation for extreme values of the invariant mass of the recoiling hadronic system.

Production measurements of ψ(2S) and X(3872) at ATLAS (4)

- The fit of the measured ratio to that template allows to determine the ratio of the average branching fractions:

$$R_B^{1L} = \frac{Br(B \to X(3872))Br(X(3872) \to J/\psi\pi^+\pi^-)}{Br(B \to \psi(2S))Br(\psi(2S) \to J/\psi\pi^+\pi^-)} = (3.95 \pm 0.32(\text{stat}) \pm 0.08(\text{sys}))\%$$

- The somewhat falling trend shown on the right figure on the previous slide does not completely agree with the shape of the template, also possibly suggesting the presence of an additional contribution to the non-prompt X(3872) yield in the low-p_T bins.
- The short-lived component is understood to be due to B_c decays, and the value of the pseudo-proper-lifetime parameter of the short-lived component is based on the value expected for B_c.
- An alternative fit model hence was implemented in the analysis, which allows for two non-prompt contributions with distinctly different effective lifetimes.

$$R_B^{2L} = \frac{Br(B \to X(3872))Br(X(3872) \to J/\psi\pi^+\pi^-)}{Br(B \to \psi(2S))Br(\psi(2S) \to J/\psi\pi^+\pi^-)} = (3.57 \pm 0.33(\text{stat}) \pm 0.11(\text{sys}))\%$$

Production measurements of ψ(2S) and X(3872) at ATLAS (5)

- Ratio of cross section times branching fraction between X(3872) and ψ(2S) for prompt (left) and non-prompt (right) production. For the non-prompt production, the total ratio is separated into short-lived and long-lived components for the X(3872).

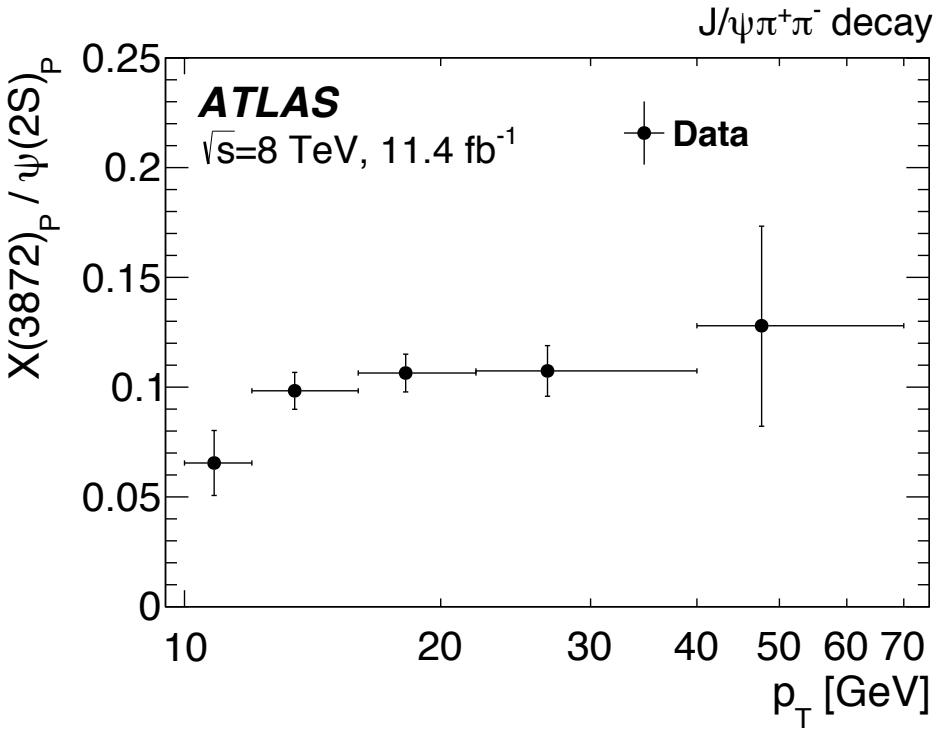

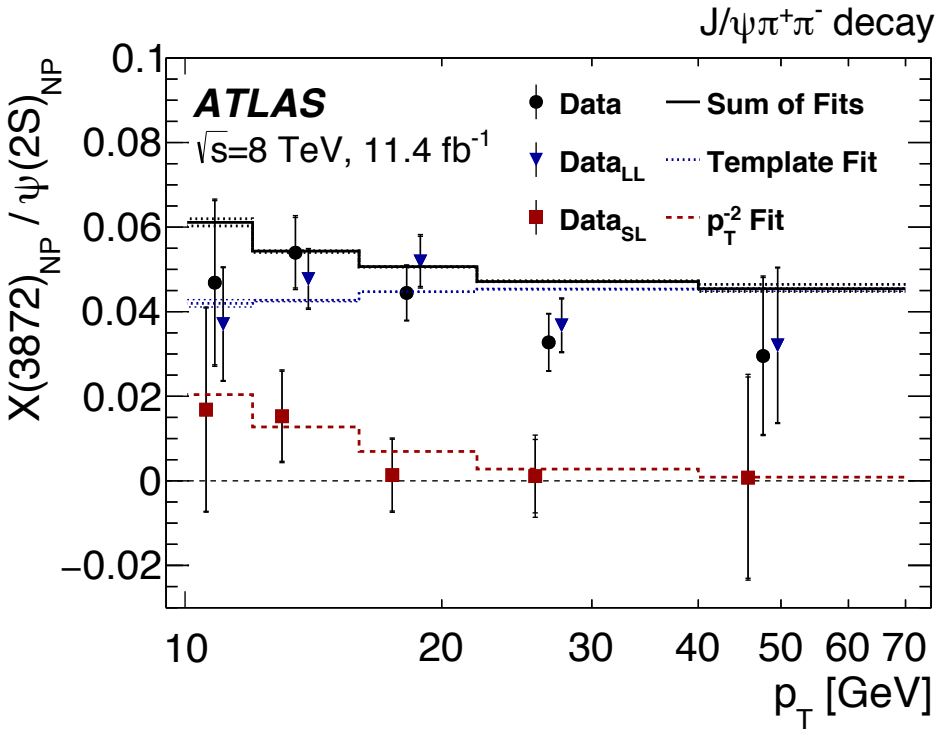

Production measurements of ψ(2S) and X(3872) at ATLAS (6)

- The above is used to determine the fraction of non-prompt X(3872) from short-lived sources, integrated over the p_T range (p_T > 10 GeV) covered in the analysis:

$$\frac{\sigma(pp \to B_c)Br(B_c \to X(3872))}{\sigma(pp \to \text{non-prompt } X(3872))} = (25 \pm 13(\text{stat}) \pm 2(\text{sys}) \pm 5(\text{spin}))\%$$

- The invariant mass distributions of the di-pion system in ψ(2S) → J/ψπ⁺π⁻ and X(3872) → J/ψπ⁺π⁻ decays are also measured. The results do not favour a phase space distribution in either decay, and favour X(3872) → J/ψρ⁰ .

Production measurements of ψ(2S) and X(3872) at ATLAS (7)

- Measured non-prompt fractions for ψ(2S) (left) and X(3872) (right) production, compared to CMS results at √s = 7 TeV.

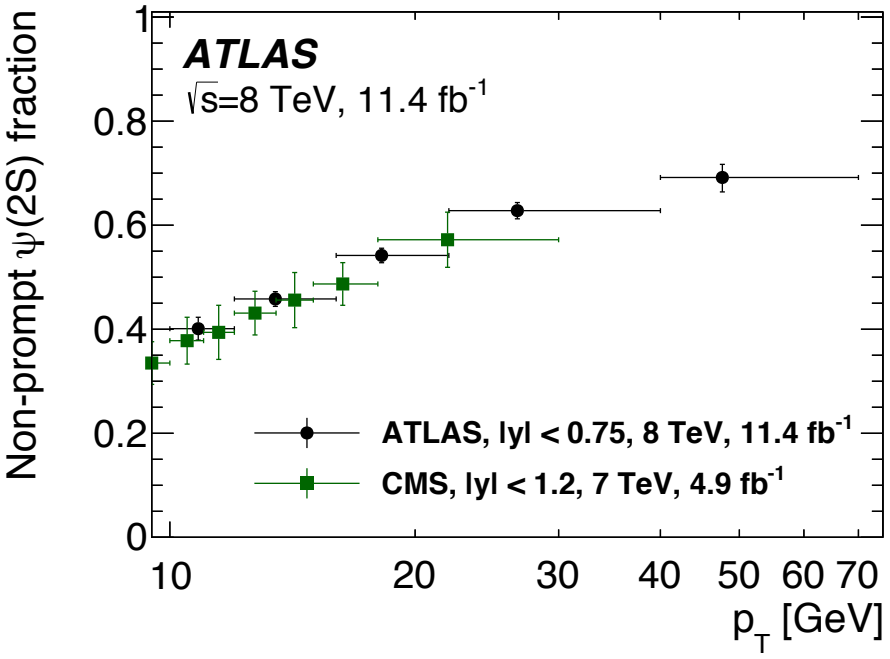

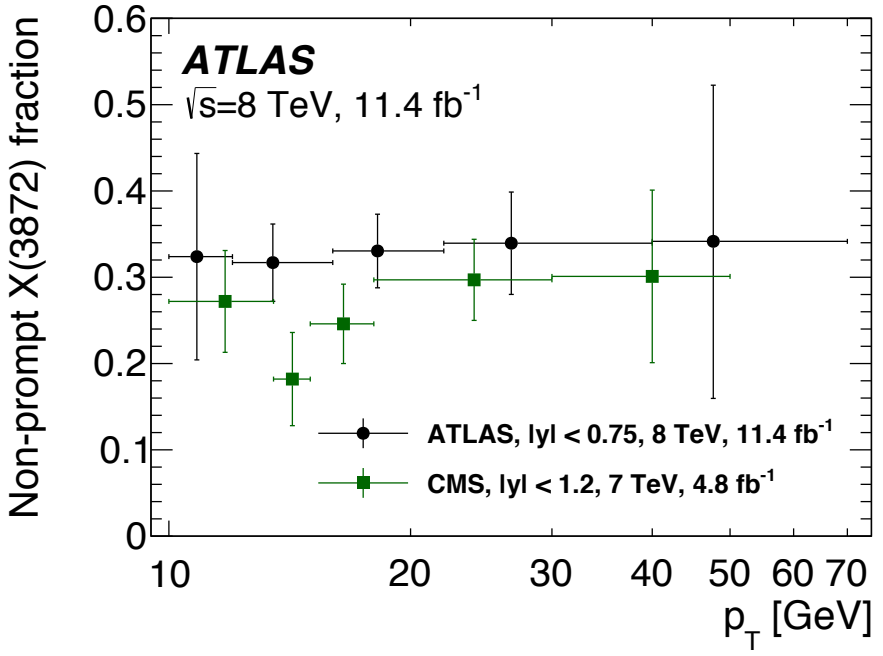

Production measurements of ψ(2S) and X(3872) at ATLAS (8)

- The measured differential cross section (times the product of the relevant branching fractions) for prompt production of ψ(2S) is presented on the left, and the non-prompt production is presented on the right. Compared to various theoretical models.

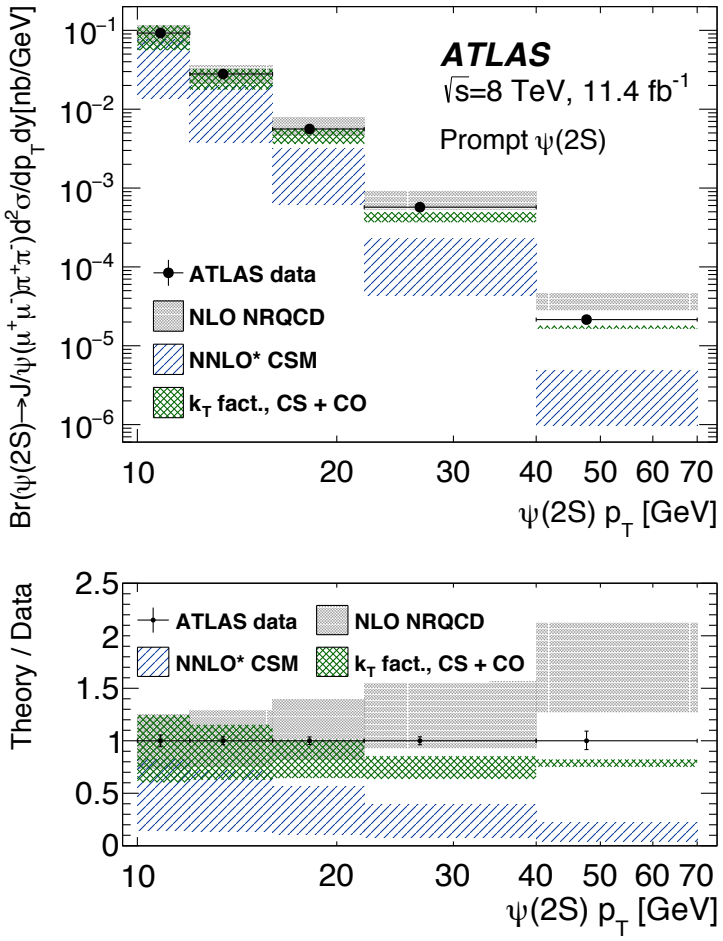

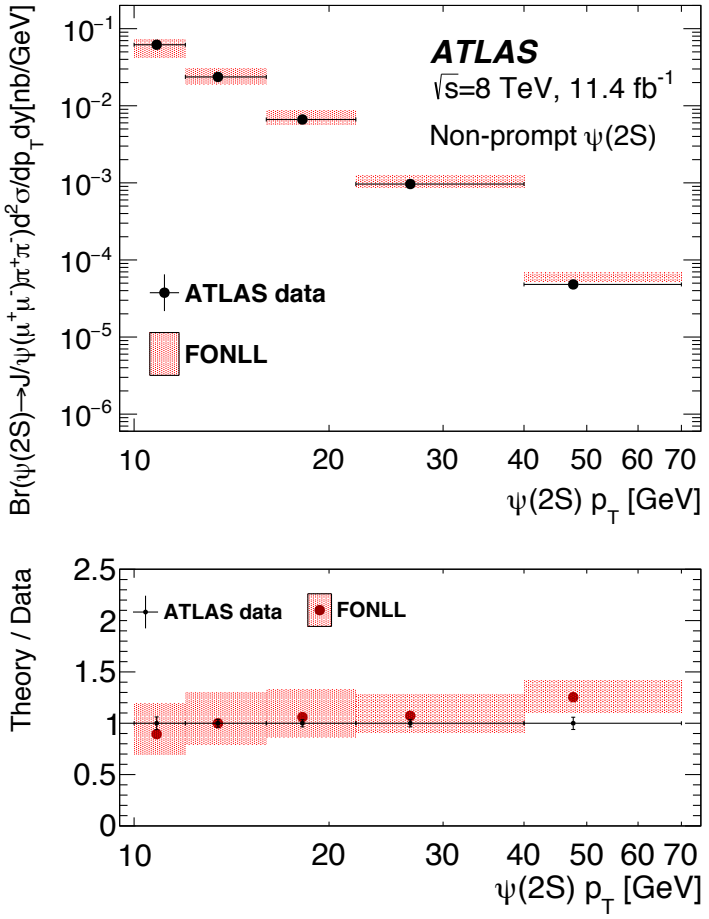

Production measurements of ψ(2S) and X(3872) at ATLAS (9)

- The measured differential cross section (times the product of the relevant branching fractions) for prompt production of X(3872) is presented on the left, and the non-prompt production is presented on the right. The X(3872) is modeled as a mixture of a $\chi_{c1}(2P)$ and a $\bar{D}^0 D^{*0}$ molecular state.

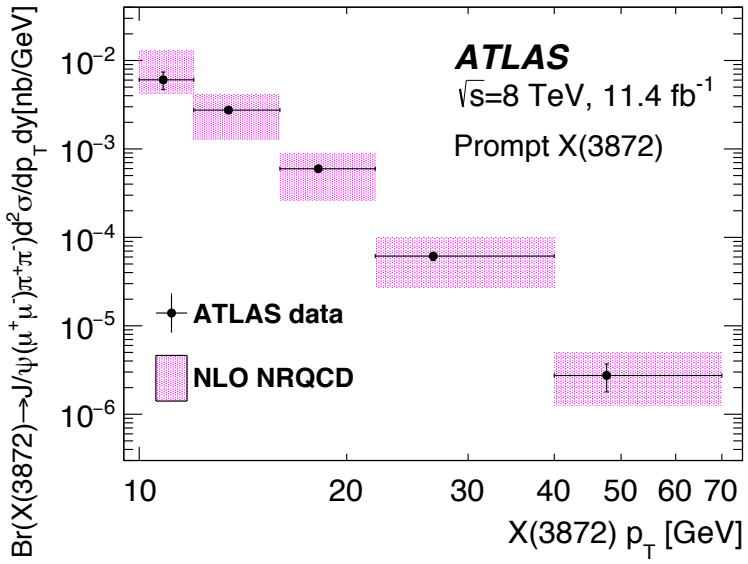

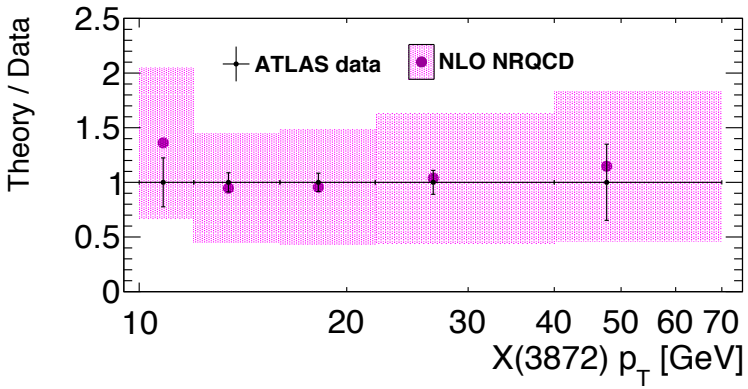

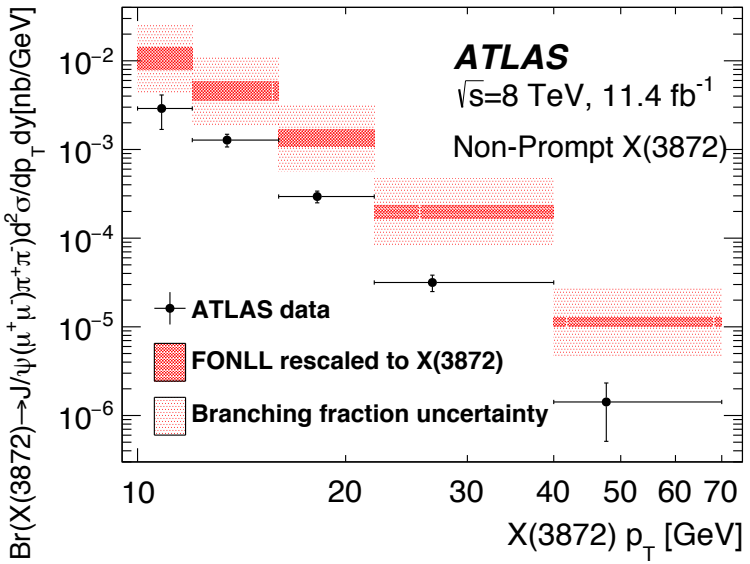

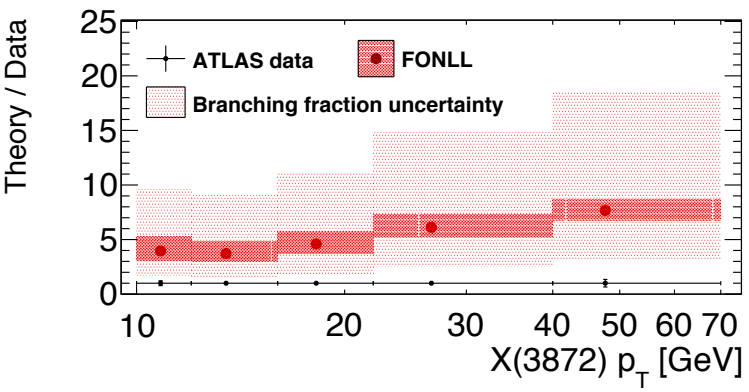

Conclusions

- $B_c(2S)$ has been observed for the first time. Mass and decay mode are consistent with theoretical expectations.
- $B_c^+ \to J/\psi D_s^+$ and $B_c^+ \to J/\psi D_s^{*+}$ decays have been studied. Four relative branching fractions were measured, theoretical predictions are within 2σ.
- X_b has been sought in $X_b \to \Upsilon(1S)\pi\pi$. No signal has been observed and upper limits have been set.
- Decay $\Lambda_b^0 \to \psi(2S)\Lambda^0$ has been observed for the first time. Measured ratio $\Gamma(\Lambda_b^0 \to \psi(2S)\Lambda^0)/\Gamma(\Lambda_b^0 \to J/\psi\Lambda^0)$ exceeds the only available theoretical prediction.
- $X(3872) \to J/\psi\pi^+\pi^-$ decay has been studied. It was found that the molecular tetraquark component is not needed in description of the prompt production. The indication of enhanced contribution of B_c to the non-prompt production has been revealed.

BACKUP

ATLAS detector

- Subsystems essential for B-physics: Inner detector and Muon spectrometer.
- Inner detector: tracking, momentum and vertexing, $|\eta|<2.5$, d_0 resolution ~10μm.
- Muon spectrometer: trigger and muon identification, $|\eta|<2.7$.
- J/ψ mass resolution: 60±1 MeV, ϒ(1S): 119±1 MeV.

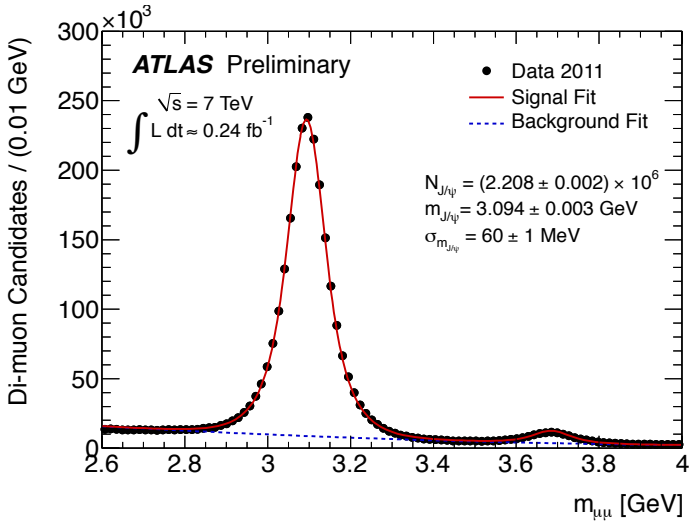

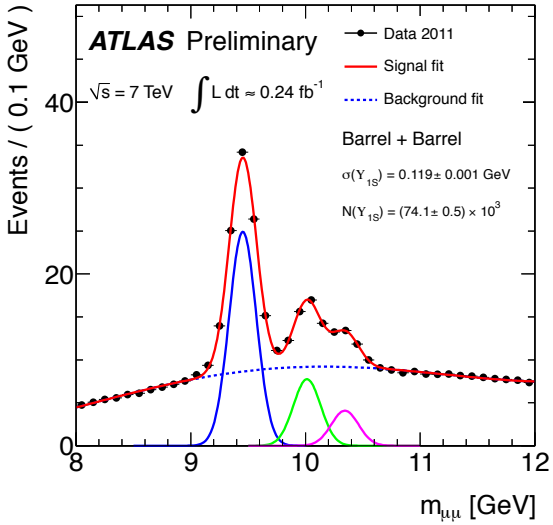

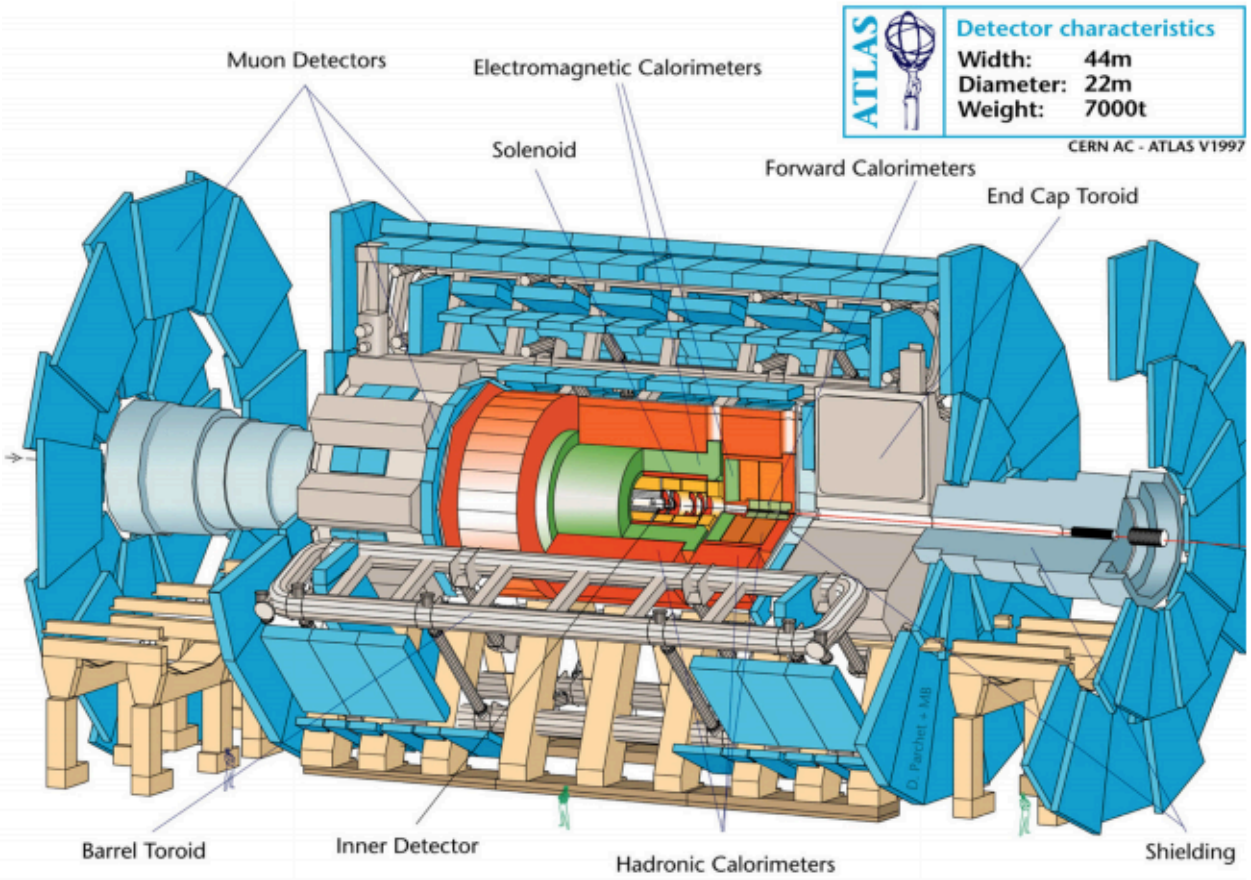

Trigger and datasets

- B-physics starts with single or di-muon triggers with various thresholds:
  - $p_T(\mu) > 6$ GeV
  - $p_T(\mu) > 18$ GeV
  - $p_T(\mu_1) > 4$ GeV & $p_T(\mu_2) > 4$ GeV
  - $p_T(\mu_1) > 6$ GeV & $p_T(\mu_2) > 4$ GeV
  - $p_T(\mu_1) > 6$ GeV & $p_T(\mu_2) > 6$ GeV

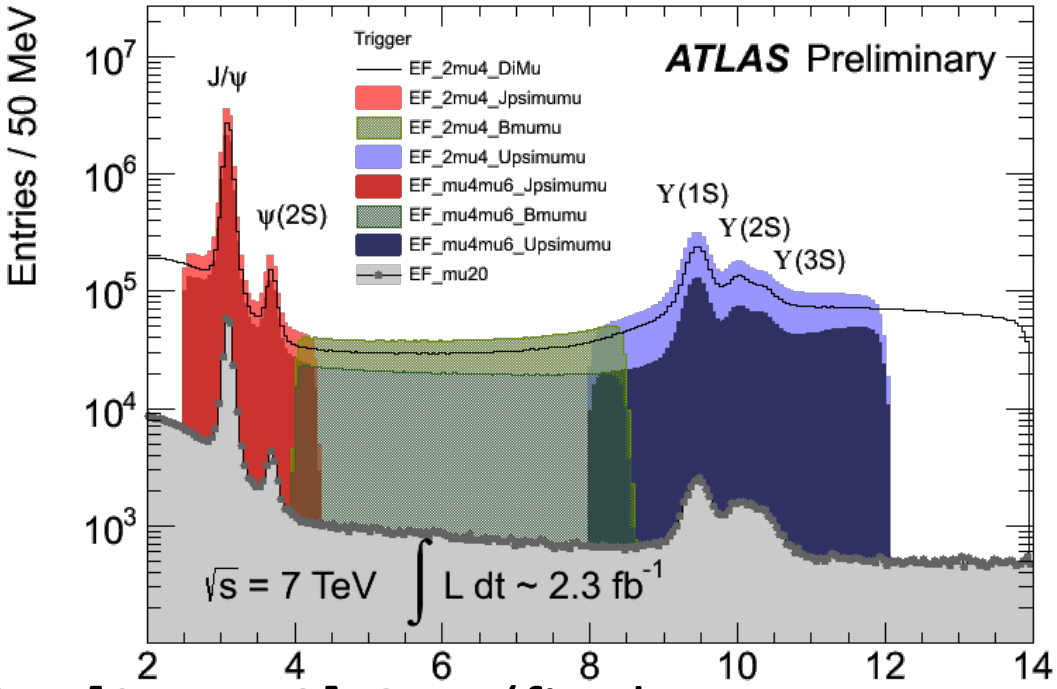

- Di-muon mass range: $m(\mu\mu) \in [2.5; 4.3]$ GeV (final states containing J/ψ) and $m(\mu\mu) \in [4.0; 8.5]$ GeV (B to μ transitions).
- No displaced vertex selection requirements: advantage for lifetime measurements.
- Datasets: 4.9 fb^{-1} @ 7 TeV and 20.6 fb^{-1} @ 8 TeV.

Production measurements of ψ(2S) and X(3872) at ATLAS (10)

- (left) Normalised differential decay width of ψ(2S) → J/ψ(→$\mu^+\mu^-$)$\pi^+\pi^-$ in bins of dipion invariant mass over the range 0.280 GeV < m(ππ) < 0.595 GeV, fitted with the Voloshin–Zakharov model. Also shown is the normalised m(ππ) phase-space distribution (red shaded histogram).
- (right) Normalised differential decay width of X(3872) → J/ψ(→$\mu^+\mu^-$)$\pi^+\pi^-$ in bins of dipion invariant mass over the range 0.28GeV < m(ππ) < 0.79GeV. Also shown is the MC prediction for the decay X(3872) → J/ψ(→$\mu^+\mu^-$)ρ^0(→ $\pi^+\pi^-$) (blue histogram) and the normalised distribution of m(ππ) phase-space (red shaded histogram).